RSC Advances

Volume 1 | Number 1 | Jan 2013 | Pages 1–100

RSC Advances

www.rsc.org/advances

ROYAL SOCIETY OF CHEMISTRY

ROYAL SOCIETY OF CHEMISTRY

www.rsc.org/advances

Degradation of phenol by air and polyoxometalate nanofibers using a continuous mode

Jian Xu[a], Siqi Yan[a], Jianxin Li[a], Shengtian Wang[a], Xiaohong Wang[a,]*, Mingxin Huo[b,]*

[a] Key Lab of Polyoxometalate Science of Ministry of Education, Faculty of Chemistry, Northeast Normal University, Changchun 130024, P. R. China

[b] School of Urban and Environmental Sciences, Northeast Normal University, Changchun 130024, P. R. China

* Corresponding author

Tel.: 0086-431-88930042; Fax: 0086-431-85099759

E-mail address: wangxh665@nenu.edu.cn

Postal address: Northeast Normal University, 5268 Renmin Street, Changchun, P. R. China

Table of content

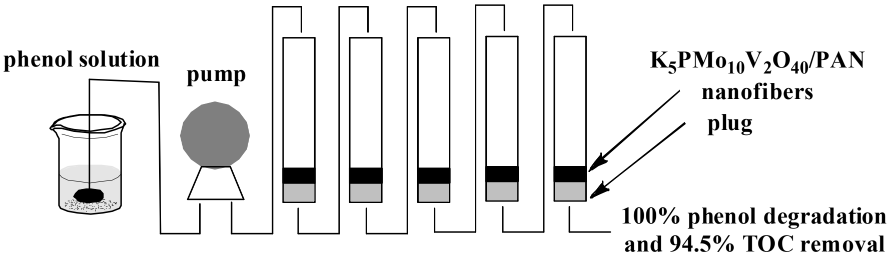

$K_5PMo_{10}V_2O_{40}$/PAN nanofibers, synthesized by electrospinning technique, were used as catalysts in phenol degradation by air under room temperature in a continuous mode. 100% degradation efficiency of phenol and 94.5% TOC removal had been obtained.

Abstract

The nanofibers were synthesized by electrospinning technique using polymer as supports and polyoxometalates (POMs) as dopants. X-ray diffraction (XRD), Fourier transform infrared (FT-IR) spectroscopy, ^{31}P MAS NMR, Scanning electron microscopy (SEM), and the high resolution transmission electron microscope (TEM) were used to characterized the resulting hybrids. These POM nanofiber catalysts could provide a continuous flowing mode to promote the oxidative degradation of phenol into simple inorganic species using air (O_2) as an oxidant at room temperature through nine cycles. The leaching of POMs from nanofibers was little, showing that the catalyst had excellent stability and could be used as heterogeneous ones.

Keywords: Polyoxometalates; Oxidation; Phenol degradation; A continuous mode; Nanofibers

1. Introduction

Phenol is an important industrial chemical because of its wide usage (e.g., disinfectant, precursor of phenolic resins, and reagent in chemical synthesis), which causes a very serious pollution because of its highly stability, low biodegradability[1], and toxicity at low concentration[2]. Many techniques based on both chemical conversions and physical operations have been used to remove phenol from wastewater including photocatalytic degradation[3], ultrasound-assisted degradation[4], catalytic wet air oxidation (CWAO)[5,6], and microwave-enhanced catalytic degradation[7,8].

In CWAO process, many catalysts had been involved including both homogeneous and heterogeneous transition-metal catalysts (Cu^{2+}, Fe^{3+}, or Mn^{2+})[9-12], and polyoxometalates[13,14]. POMs are very available for CWAO of phenol due to the outstanding redox behavior and unique Keggin structure. The major limitation of such POM catalysts is their low surface area, high solubility in polar solvents, and thermal instability. Therefore, many attempts have been made to transfer homogeneous state into heterogeneous one by supporting them on different carriers[15,16]. S. W. Kim's group reported $H_5PMo_{10}V_2O_{40}$ supported on silica ball/mesoporous carbon/SBA-15 as heterogeneous catalyst in CWAO of phenol[13] using H_2O_2 as an oxidant. The alternative way is to integrate POMs into polymer matrices, which is a good method to create novel POM-containing polymers possessing the unique properties of POM clusters and the favorable processability of polymers[17]. Meanwhile, fiber polymeric membranes have been shown to be very useful for heterogeneous catalysis[18] and micro-filters[19], which give the potential application in removing organic pollutions from wastewater. More importantly, one dimensional (1D) nanofibers can make catalytic fiber membranes available for a continuous mode by passing the pollutant solution through the membrane, which is suitable for industrial applications. Electrospinning is an effective and easily controllable way to fabricate POM/polymer nanofibers compared to other methods[20], which could only use the simple mixed solution of polymer and POM precursors to fabricate 1D nanofibers with long length, uniform diameter, diverse composition, and high surface, which can be applied in many fields such as catalyst supports. By now, there were few reports on the construction of one-dimensional POM nanofibers using electrospinning method[21-24], which only one had been used in photodegradtion of organic dye. The aim of the present work is to fabricate POM functionalized fiber membranes using simple procedure, and to develop a novel technology for decontamination of industrial wastewaters and polluted water resources based on POMs. Therefore, the electrospinning technique was used to fabricate POM nanofibers using insoluble polymer as support. The hybrid catalysts were used to evaluate the catalytic activity for CWAO of phenol on a continuous mode. By now, there is no report on the degradation of phenol using a continuous mode based on POM catalysts.

2. Results and discussion

2.1. Characterization of $K_5PMo_{10}V_2O_{40}$/PAN nanofibers

From the result of elemental analysis, the each contents of $K_5PMo_{10}V_2O_{40}$/PAN were Mo, 7. 05; P, 0.22; V, 0.75; and C, 49.45%, respectively. It can be seen that the molar ratio of Mo : P : V was 10 : 1 : 2, showing that POMs was intact in polymer fibers. Meanwhile, the content of $K_5PMo_{10}V_2O_{40}$ in PAN was 14.2%.

The IR spectrum of POM nanofibers was investigated (Fig. 1a). Peaks in the range of 600-1100 cm^{-1} could be easily distinguished with 1084, 949, 852, and 797 cm^{-1}, respectively. Its parent $[PMo_{10}V_2O_{40}]^{5-}$ gives four characteristic peaks including P-O stretching (~1064 cm^{-1}), M-O_{ter} stretching (~964 cm^{-1}), Mo-O_c-Mo stretching of inter bridges between corner-sharing MoO_6 octahedra (~876 cm^{-1}), and Mo-O_e-Mo stretching of intra bridges between edge-sharing MoO_6 octahedra (~814 cm^{-1}). From the IR results, POMs kept its original Keggin structure after being loaded on PAN. The peak at 2294 cm^{-1} was attributed to $C \equiv N$ corresponding to PAN. Meanwhile, some shifts indicated the interaction between POM and PAN polymer.

The ^{31}P MAS NMR spectrum of $K_5PMo_{10}V_2O_{40}$/PAN was recorded (Fig. 1b). It can be seen that two signal peaks at 5.61 and 6.56 ppm for $K_5PMo_{10}V_2O_{40}$/PAN, respectively. Compared to its parent $K_5PMo_{10}V_2O_{40}$ (δ = 4.75 ppm), the split of one peak into two was attributed to the interaction between $K_5PMo_{10}V_2O_{40}$ and polymer PAN.

Fig.1c gave a typical SEM image of the $K_5PMo_{10}V_2O_{40}$/PAN nanofibers with an average diameter of 100 nm. From the EDS (Fig.1d), the molar ratio of P, Mo and V was 1 : 10 : 2. From the image of high resolution TEM (Fig. 1e), it can be seen that $K_5PMo_{10}V_2O_{40}$ dispersed uniformed around the polymer.

Fig. 1

From the result of elemental analysis (Mo, 8.39; P, 0.24; V, 0.45; and C, 47.23%, respectively), the molar ratio of Mo : P : V was 11 : 1 : 1, showing that the original structure had been kept. Meanwhile, the content of $K_4PMo_{11}VO_{40}$ in PAN was 16.0%. From the SEM image of $K_4PMo_{11}VO_{40}$/PAN (Fig. 1f), it can be seen the diameter was about 100 nm.

2.2. CWAO activity of $K_5PMo_{10}V_2O_{40}$/PAN nanofibers

Firstly, in order to determine the catalytic activity of $K_5PMo_{10}V_2O_{40}$/PAN, the degradation of phenol by different catalysts had been done (Fig. 2) under flowing oxygen in a flash reactor. It can be seen that no phenol degradation was detected without any catalyst, which meant that the oxidation ability of O_2 at room temperature was limited. The catalytic activity was arranged as followings: $K_4PMo_{11}VO_{40} < K_5PMo_{10}V_2O_{40} < K_4PMo_{11}VO_{40}/PAN < K_5PMo_{10}V_2O_{40}/PAN$. The potassium of POMs is insoluble in water at room temperature and owns small surface area of 4.3 m^2/g, which acted as a heterogeneous catalyst. $K_5PMo_{10}V_2O_{40}$ exhibited low activity in degradation of phenol by air. The highest activity was obtained by $K_5PMo_{10}V_2O_{40}$/PAN, which exhibited 96.4% degradation efficiency for 0.72 mM phenol as three times higher as $K_5PMo_{10}V_2O_{40}$ did. The higher activity of $K_5PMo_{10}V_2O_{40}$/PAN was attributed to the high dispersion of $K_5PMo_{10}V_2O_{40}$ on PAN nanofibers, high surface area, the enhanced adsorption of phenol by PAN. From its XRD (Fig. S1), no POM diffraction peaks were observed, indicating the good disperse of $K_5PMo_{10}V_2O_{40}$ around PAN nanofibers. The image of high resolution TEM also determined the uniformed dispersion of $K_5PMo_{10}V_2O_{40}$. The surface area of $K_5PMo_{10}V_2O_{40}$/PAN was about 361.8 m^2/g higher than that of $K_5PMo_{10}V_2O_{40}$. It is known that the nanofiber membrane can adsorb some substrates. The adsorption capacity on oxidation catalyst is a key factor for the degradation rate in air oxidation process[25], which provides enhanced mass transport for oxygen molecules into and out of the pore structure[26]. The adsorptions of phenol by $K_5PMo_{10}V_2O_{40}$/PAN and $K_5PMo_{10}V_2O_{40}$ were about 24.5 and 3.6%, respectively. The increasing adsorption of phenol was attributed to the effect of PAN (23.9%). Therefore, it can be concluded that the adsorption of phenol had been enhanced by assistance of PAN nanofibers, hence to enlarge the degradation rate. In addition, the content of vanadium in POMs also influenced the degradation of phenol, that was, monovanadium POM $K_4PMo_{11}VO_{40}$/PAN exhibited lower activity than divanadium

$K_5PMo_{10}V_2O_{40}$/PAN did. Cyclic voltammetry of $K_4PMo_{11}VO_{40}$/PAN and $K_5PMo_{10}V_2O_{40}$/PAN gave the first redox potentials for the VO_2^+/VO^{2+} couple in water as 0.46, and 0.47 V, respectively. Therefore, the different catalytic performance was supposed to correspond to the redox potential with respect to vanadium substitution similar to our previous report[27].

Fig. 2

It is important to clarify that the removal of phenol by $K_5PMo_{10}V_2O_{40}$/PAN was through adsorption or through oxidation. Therefore, the degradation products during the reaction had been determined (Fig. S2) using ion chromatography and HPLC. It can be seen that phenol was firstly oxidized into hydroquinone, catechol, and then p-benzoquinone, o-benzoquinone, and maleric acid. The final degradation products were CO_2 and water, which could be determined by $Ca(OH)_2$. These results could determine that the removal of phenol was through oxidative process by air and catalyzed by $K_5PMo_{10}V_2O_{40}$/PAN.

To study the effect of initial concentration on the degradation of phenol, experiments were carried out with different concentrations of phenol from 0.72 mM to 3.60 mM (Fig. S3a). It was found that with increase in concentration of phenol, the degradation efficiency decreased, which showed that the phenol removal depended on its initial concentration. The decreasing of activity was attributed to the decreasing ratio of phenol to catalyst, showing that the limitation of catalytically active sites hindered the further adsorption of phenol resulting in lower activity. In addition, the influence of the temperature on degradation efficiency was done (Fig. S3b). It can be seen that the degradation efficiency increased by increasing temperature from 0ºC to 25ºC. Meanwhile, the catalytic activity of $K_5PMo_{10}V_2O_{40}$/PAN was high even at a lower temperature, where the degradation efficiency is 82.4% for a 120 min reaction. The amount of catalyst also influenced the degradation of phenol (Fig. S3c), while 0.2 g of $K_5PMo_{10}V_2O_{40}$/PAN could give 96.4% removal of phenol.

Based on the above results, it can be concluded that the removal of phenol by $K_5PMo_{10}V_2O_{40}$/PAN and oxygen underwent the two steps: initially, the reactants (phenol and dioxygen) reached the surface of nanofibers and were adsorbed on the surface by hydrogen bonding interactions between the hydroxyl groups from phenol and the oxygen atoms from the POMs. Secondly, phenol molecules was oxidized by some free radicals, which had been already studied by our group[27]. This process was influenced by the adsorption of phenol on the nanofibers, the generation of free radicals, the usage of the catalyst or oxygen, and temperature.

2.3 The degradation of phenol using continuous mode

The degradation of phenol under continuous mode is more convenient for coupling and separation. Therefore, the degradation efficiency of phenol at different flow rates had been summarized in Fig. 3 using a continuous mode. The results indicated that with decreasing flow rate from 14.4 to 4.8 mL/min, removal efficiency increased from 70.7% to 100% for nine cycles. The cycling times of total degradation of phenol were different when using different flow rates 14.4, 9.6, and 4.8 mL/min with 9, 12 and 14, respectively. Using a slow flow rate, the residence time of the reactant in the reactor increased, which resulted in high degradation efficiency. Compared to the result of placing all of the catalyst in one tube (the final decolorization effect was about 87.8%), the tandem of nine glass tubes might provide better performance. It might be attributed to the residence time of phenol molecules on the surface of catalyst. In our experimental conditions, the usage of the catalyst was small, so all of catalyst was put in one tube, the time of the dye molecules flowing across the catalyst fibers was relative shorter than in nine tandem tubes. Therefore, the continuous mode might be more available for treating phenol waste water.

Fig. 3

The initial concentration of phenol also influenced the degradation effect, while experiments were carried out with different concentrations of phenol from 0.72 mM to 3.6 mM (Fig. 4) at flowing rate of 4.8 mL/min. It is found that with increase in concentration of phenol from 0.72 to 2.88 mM, the degradation efficiency decreased.

Fig. 4

Mineralization of phenol in a continuous mode was studied by COD (chemical oxygen demand), and TOC (total organic carbon) assay. COD values have been related to the total concentration of organics in the solution and the decrease of COD reflects the degree of mineralization[28]. Significant decrease of COD was observed as 95.8%. The TOC reduction of phenol reached 94.5% after ninth glass. Total mineralization could be achieved by $K_5PMo_{10}V_2O_{40}$/PAN and air, which showed that it was catalytically active and suitable for mineralization of phenol in a continuous mode.

The IR spectrum of $K_5PMo_{10}V_2O_{40}$/PAN after the reaction showed no changes, showing that its stability during the reaction. Meanwhile, no peaks corresponding to phenol indicated that no phenol adsorbed on the surface of catalyst. The phenol was totally degraded into CO_2 and water. The leaching of $K_5PMo_{10}V_2O_{40}$ was 1.8 ppm in the continuous mode, showing little leaching of catalytic sites from the polymer supports.

Reusability of the catalysts is very important for heterogeneous POM nanofibers. After first catalytic run, the hybrid nanofibers were washed with distilled water in reactor and dried under air for reuse. Two catalytic cycles were accomplished successfully with almost same activity with no observable loss in its performance.

3. Experimental

3.1. Materials

Polyacrylonitrile (PAN, Mw = 150,000) was purchased from Aldrich. And other reagents were of AR grade and used without further purification. For oxidation degradation, 0.1 M stock solution of phenol was prepared and aqueous solution of needed concentration was prepared from the stock solution. Molybdovanadophosphoric salts ($K_5PMo_{10}V_2O_{40}$ and $K_4PMo_{11}VO_{40}$) were prepared according to the refs 29, and were characterized by IR spectroscopy.

3.2. Apparatus

Elemental analysis was carried out using a Leeman Plasma Spec (I) ICP-ES (Leeman LABs. Inc.). IR spectra (4000-500 cm^{-1}) were recorded in KBr discs on a Nicolet Magna 560 IR spectrometer. SEM was operated using XL30 ESEM FEG at 25kV (Philips XL-30). The high resolution TEM image was measured on JOEL JEM-2100F microscope. XRD patterns of the sample were collected on a Rigaku D_{max} 2000 X-ray diffractometer with Cu K_α radiation (λ = 0.154178 nm) (Rigaku Corporation). The ^{31}P MAS NMR measurements were obtained using a Bruker AM500 spectrometer at 202.5 MHz. Nitrogen porosimetry was performed on a Micromeritics ASAP 2010 instrument. Surface areas were calculated using the BET equation. Analysis of phenol and intermediates during the reaction was performed by High Performance Liquid Chromatography (HPLC, Shimadzu LC-20A) with a UV detector using a Shim-pack VP-ODS (4.6 mm×250 mm, 5 μm) column. A DX-300 ion chromatography (IC) equipped with a conductivity detector and an ICE-ASI anion column was also used to determine the changes of the concentrations of the intermediates and final products. Total organic carbon (TOC) was monitored using a Shimadzu TOC-VCPH total organic carbon analysis system. Chemical oxygen demand (COD) was determined by a closed reflux colorimetric method using 756 CRT UV-vis spectrophotometer at a wavelength of 600 nm. The leaching concentrations of $K_5PMo_{10}V_2O_{40}$ during the reaction were also measured through analyzing the dissolved concentration of Mo in aqueous solution using a Leeman Plasma Spec (I) ICP-ES. The cyclic voltammograms were recorded with an RDK-RW-117 X-Y recorder (Japan).

3.3. Preparation of $K_5PMo_{10}V_2O_{40}$/PAN nanofibers

Nanofibers of $K_5PMo_{10}V_2O_{40}$/PAN were prepared by a method of electrospinning technique. A 10 wt. % polymer solution was prepared by adding 1.85 g PAN into 16.65 g of (N,N-Dimethylformamide) DMF with stirring for 5 h at 60°C. 0.27 g of $K_5PMo_{10}V_2O_{40}$ was added into the above solution with gentle stirring for 12 h to obtain a homogeneous hybrid sol for further electrospinning.

The preparation of $K_4PMo_{11}VO_{40}$/PAN was used the same method except $K_4PMo_{11}VO_{40}$ instead of $K_5PMo_{10}V_2O_{40}$.

3.4. Catalytic Activity

For slurry-type reactors, a certain amount of catalysts was suspended in a fresh aqueous phenol solution (C_0 = 0.72 mM, 100 mL, pH = 1.7) in three-neck glass flask at ambient temperature (25°C). The air was inputted into the bottom of the suspension with the flowing rate 0.04 m^3/h. This process uses oxygen dissolved in the aqueous solution as an oxidant directly. Oxygen concentration depends on the oxygen solubility at room temperature and atmospheric pressure. Samples were withdrawn periodically to be measured. After finishing, the catalyst was separated by filtration and washed with water for three times to be reused.

The continuous experiments were carried out in a continuous-flow reactor, which was shown in Scheme 1. The reactor comprised five glass tubes (inner diameter 25 mm, outer diameter 26.6 mm), which were serially connected by means of transparent polyethylene tubes from the top to the bottom. Each glass tube was equipped with a permeable plug at the base of a glass tube. The $K_5PMo_{10}V_2O_{40}$/PAN (0.2 g) fibers were fixed on top of the plug. The oxygen-saturated solution was obtained by bubbling with air for at least 20 min. 100 mL of phenol solution (0.72 mM) was then forced through the membrane with different rate at room temperature (25 ºC). A sample was collected from the outlet of each glass column.

Scheme 1

3.5. Adsorption experiments

For the adsorption measurements, 100 mL, 0.72 mL of freshly prepared phenol solution passed through $K_5PMo_{10}V_2O_{40}$/PAN fibers (0.2 g) at flowing rate of 4.8 mL/min by bubbling with N_2 to drive out dissolved O_2. Until all the solution passed through the membrane, a sample was taken to determine phenol' concentration.

4. Conclusion

The present study reported the fabrication of POMs/PAN nanofibers by electrospinning technique, and they were employed as catalysts for degradation of phenol in a continuous mode at room temperature. $K_5PMo_{10}V_2O_{40}$/PAN nanofibers exhibited excellent catalytic activity due to its unique property such as high disperse of POM, high surface area, and enhanced adsorption of phenol. Phenol molecules were completely mineralized into small inorganic species CO_2 and water at nine tandem glass tubes. This catalytic process showed to be a commercial and green chemical pathway with potential industrial application in phenol degradation.

Acknowledgements

This work was supported by the National Natural Science Foundation of China (No. 51078066), the major projects of Jilin Provincial Science and Technology Department (20086035, 20100416, and 201105001).

References

[1] N. S. Inchaurrondo, P. Massa, R. Fenoglio, J. Font, P. Haure, *Chem. Eng. J.*, 2012, **198-199**, 426-434.

[2] M. A. Baboli, *Environ. Toxicol. Phar.*, 2012, **34**, 826-831.

[3] R. Mu, Z. Xu, L. Li, Y. Shao, H. Wan, S. Zheng, *J. Hazard. Mater.*, 2010, **176**, 495-502.

[4] E. V. Rhokina, E. Repo, J. Virkutyte, *Ultrason. Sonochem.*, 2010, **17**, 541-546.

[5] M. H. El-Naas, S. Al-Zuhair, S. Makhlouf, *Chem. Eng. J.*, 2010, **160**, 565-570.

[6] F. Arena, C. Italiano, A. Raneri, C. Saja, *Appl. Catal. B: Environ.*, 2010, **99**, 321-328.

[7] L. T. Lai, C. C. Lee, G. L. Huang, Y. Y. Shu, C. B. Wang, *Appl. Catal. B: Environ.*, 2008, **78**, 151-157.

[8] B. Y. Jibril, A. Y. Atta, Y. M. Al-Waheibi, T. K. Al-Waheibi, *J. Ind. Eng. Chem.*, 2013, **19**, 1800-1804.

[9] M. Abecassis-Wolfovich, M. V. Landau, A. Brenner, M. Herskowitz, *Ind. Eng. Chem. Res.*, 2004, **43**, 5089-5097.

[10] M. Abecassis-Wolfovich, R. Jothiramalingam, M. V. Landau, M. Herrskowitz, B. Viswanathan, T. K. Varadarajan, *Appl. Catal. B: Environ.*, 2005, **59**, 91-98.

[11] F. Arena, J. Negro, G. Trunfio, A. Parmaliana, *Ind. Eng. Chem. Res.*, 2007, **46**, 6724-6731.

[12] F. Arena, G. Trunfio, J. Negro, L. Spadaro, Appl. *Catal. B: Environ.*, 2008, **85**, 40-47.

[13] S. V. Mayani, V. J. Mayani, S. W. Kim, *Mater. Lett.*, 2013, **111**, 112-115.

[14] S. Zhao, X. H. Wang, M. X. Huo, *Appl. Catal. B: Environ.*, 2010, **97**, 127-134.

[15] K. M. Parida, S. Mallick, *J. Mol. Catal. A: Chem.*, 2008, **279**, 104-111.

[16] K. Y. Lee, S. Oishi, H. Igarashi, M. Misono, *Catal. Today*, 1997, **33**, 183-189.

[17] W. K. Miao, Y. K. Yan, X. L. Wang, Y. Xiao, L. J. Ren, P. Zheng, C. H. Wang, L. X. Ren, W. Wang, *ACS Macro Lett.*, 2014, **3**, 211-215.

[18] H. Yu, J. Zhu, Y. G. Li, Q. H. Zhang, M. F. Zhu, *Mater. Lett.*, 2012, **74**, 247-249.

[19] K. H. Choo, D. I. Chang, K. W. Park, M. H. Kim, *J. Hazard. Mater.*, 2008, **152**, 183-190.

[20] A. Formhals, *U. S. Pat. Specif.*, 1934, **1**, 504-975.

[21] C. H. Sui, C. Li, X. H. Guo, T. X. Cheng, Y. K. Gao, G. D. Zhou, J. Gong, J. S. Du, *Appl. Surf. Sci.,* 2012, **258**, 7105-7111.

[22] B. Ding, C. Li, S. Fujita, S. Shiratori, *Colloid Surf. A-Physicochem. Eng. Asp.*, 2006, **284-285**, 257-262.

[23] J. Gong, X. Li, B. Ding, D. R. Lee, H. Y. Kim, *J. Appl. Polym. Sci.*, 2003, **89**, 1573-1578.

[24] J. Gong, C. Shao, Y. Pan, F. M. Gao, L. Y. Qu, *Mater. Chem. Phys.*, 2004, **86**, 156-160.

[25] M. W. Xue, X. D. Gu, J. P. Chen, H. L. Zhang, J. Y. Shen, *Themochim. Acta.*, 2005, **434**, 50-54.

[26] Y. Yang, Q. Y. Wu, Y. H. Guo, C. W. Hu, E. B. Wang, *J. Mol. Catal. A: Chem.*, 2005, **225**, 203-212.

[27] S. Zhao, X. H. Wang, M. X. Huo, *Appl. Catal. B: Environ.*, 2010, **97**, 127-134.

[28] M. A. Behnajady, N. Modirshahla, N. Daneshvar, M. Rabbani, *J. Hazard. Mater.*, 2007, **140**, 257-263.

[29] G. A. Tsigdinos, C. J. Hallada, *Inorg. Chem.*, 1968, **7**, 437-441.

Figure captions

Fig. 1. (a) The IR spectrum of $K_5PMo_{10}V_2O_{40}$/PAN nanofibers; (b) ^{31}P MAS NMR of $K_5PMo_{10}V_2O_{40}$/PAN nanofibers; (c) SEM image of $K_5PMo_{10}V_2O_{40}$/PAN nanofibers; (d) EDS of $K_5PMo_{10}V_2O_{40}$/PAN nanofibers; (e) The high resolution TEM of $K_5PMo_{10}V_2O_{40}$/PAN nanofibe; (f) SEM image of $K_4PMo_{11}VO_{40}$/PAN nanofibers.

Fig. 2. Degradation efficiency of phenol by different catalysts (POMs 28 mg and POM nanofiber 0.2 g) at room temperature, 100 mL of 0.72 mM phenol solution, with the air flowing rate 0.04 m^3/h under slurry type.

Fig. 3. Effect of the flow rate of phenol solution on degradation under continuous mode (room temperature, 100 mL of 0.72 mM phenol solution).

Fig. 4. Effect of the phenol' concentrations on degradation efficiency with flowing rate 4.8 mL/min.

Scheme 1. Schematic diagram of tubular continuous flow reactor.

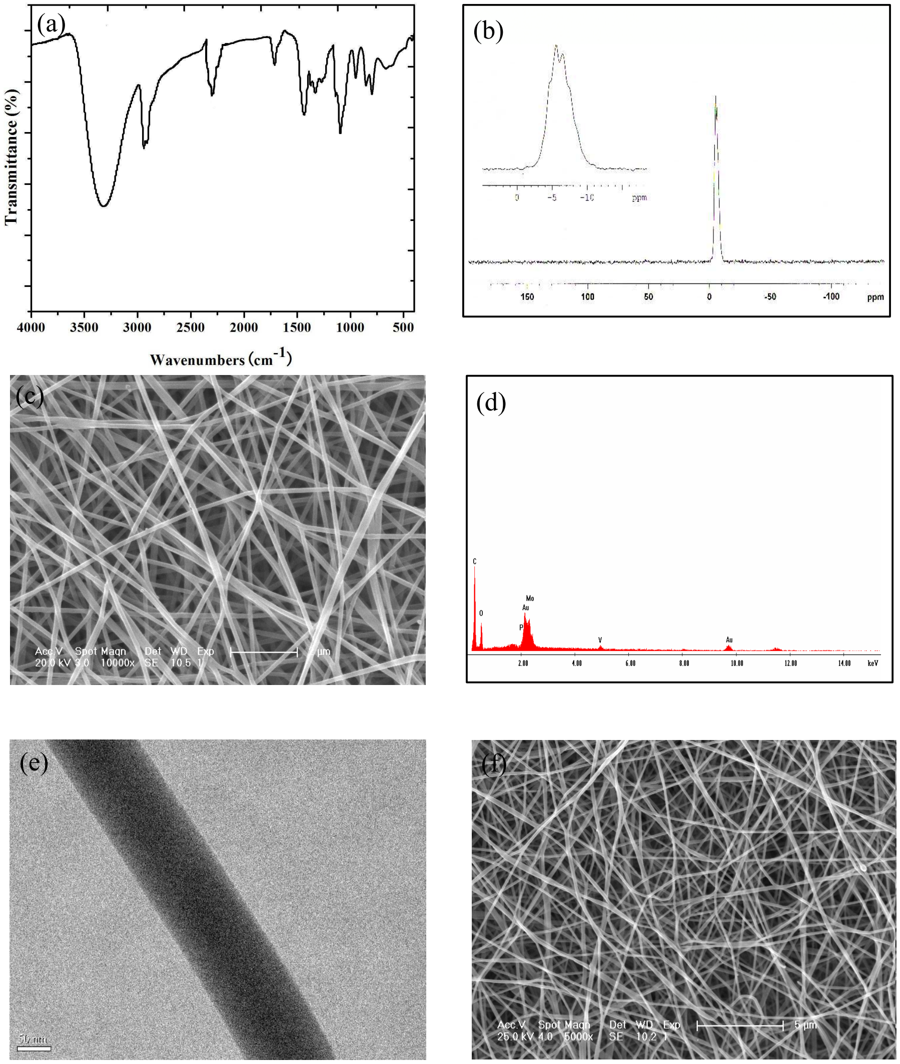

Fig. 1. (a) The IR spectrum of $K_5PMo_{10}V_2O_{40}$/PAN nanofibers
(b) ^{31}P MAS NMR of $K_5PMo_{10}V_2O_{40}$/PAN nanofibers
(c) SEM image of $K_5PMo_{10}V_2O_{40}$/PAN nanofibers
(d) EDS of $K_5PMo_{10}V_2O_{40}$/PAN nanofibers
(e) The high resolution TEM of $K_5PMo_{10}V_2O_{40}$/PAN nanofibers
(f) SEM image of $K_4PMo_{11}VO_{40}$/PAN nanofibers

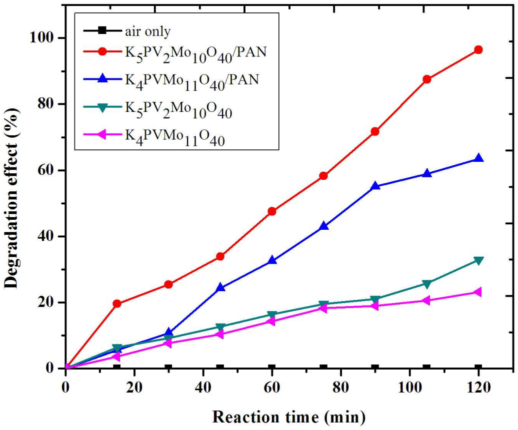

Fig. 2. Degradation efficiency of phenol by different catalysts (POMs 28 mg and POM nanofiber 0.2 g) at room temperature, 100 mL of 0.72 mM phenol solution, with the air flowing rate 0.04 m^3/h under slurry type

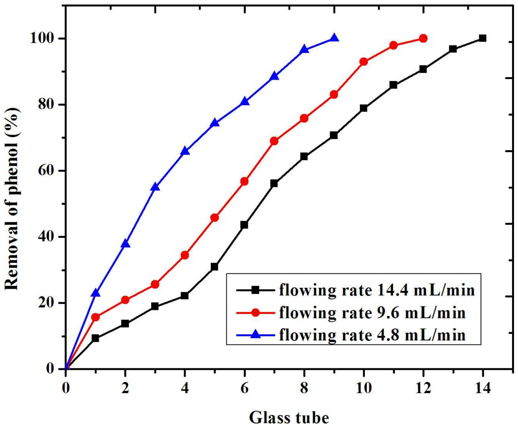

Fig. 3. Effect of the flow rate of phenol solution on degradation under continuous mode (room temperature, 100 mL of 0.72 mM phenol solution)

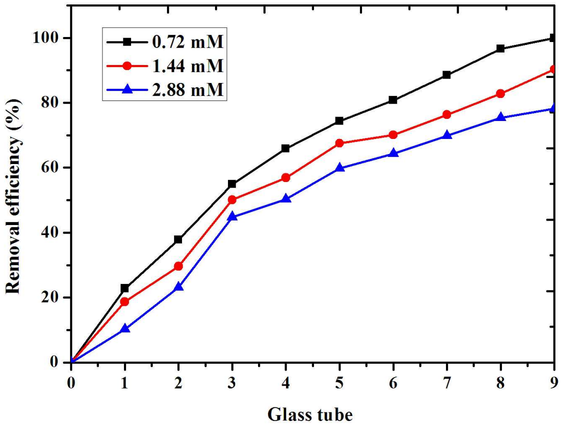

Fig. 4. Effect of the phenol' concentrations on degradation efficiency with flowing rate 4.8 mL/min

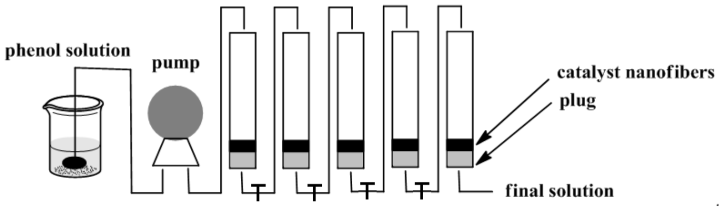

Scheme 1. Schematic diagram of tubular continuous flow reactor